

Biogenic synthesis of silver nanoparticles and investigation of antibacterial activity from leaves of *Duranta erecta*

Snehal G. Patel*  and Narendra K. Patel 

Department of Botany, Sheth M.N. Science College, Patan-Gujarat, India

Correspondence: **Snehal G. Patel**, patelsnehal2016@gmail.com

Received: 26-07-2022; Accepted: 30-11-2022; Published: 01-01-2023

DOI: [10.21608/ejar.2022.151716.1252](https://doi.org/10.21608/ejar.2022.151716.1252)



ABSTRACT

The scientific topic of nanobiotechnology is one that is expanding quickly and has potential applications in the life sciences and human healthcare. Nanomedicine and biomedical nanotechnology both heavily rely on silver nanoparticles. Silver is a precious metal that naturally occurs, most frequently as part of a mineral resource in combination with other elements. With regard to various diseases, including bacteria, fungi, viruses, and yeast, silver nanoparticles have a natural antibacterial action. In the current investigation, *Duranta erecta* leaves were used in the manufacture of silver nanoparticles. The produced silver nanoparticles were studied using UV-VIS spectra, Transmission Electron Microscopy (TEM), X-ray Diffraction (XRD), and Fourier Transfer Infrared Spectra (FTIR). The produced silver nanoparticles from *Duranta erecta* leaves were tested using the nutrient agar disk diffusion technique by four bacterial species: *E. coli*, *Streptococcus aureus*, *Bacillus subtilis*, and *Pseudomonas aeruginosa*. UV-VIS Spectra were utilized to analyze the reduced silver ions and revealed a large resonance band at 410 nm. Through XRD, intense peaks and crystalline nanoparticle production were seen. TEM interpretation revealed spherical AgNPs in a range of diameters from 6 to 16 nm. All these gram-positive (*S. aureus* and *B. subtilis*) and gram-negative (*E. Coli* and *P. aeruginosa*) bacteria produce positive findings in the current investigation.

Keywords: Plant-Mediated Silver Nanoparticles, *Duranta erecta*, TEM, XRD, Antibacterial

INTRODUCTION

Nanotechnology is a vast branch of science that deals with the synthesis, characterisation, and application of diverse nanoscale materials. It has applications in a number of fields, including chemistry, physics, material science, biology, etc. (Siddiqi *et al.*, 2018) and it is assumed that the essential elements of nanotechnology are nanoparticles (Jouyban & Rahimpour, 2020). In general, the term "nanoscale" refers to a scale between 1 and 100 nm that displays entirely new or improved properties in comparison to the bulk material that was collected based on precise features including distribution, size, form, and morphology (Yang *et al.*, 2018). In comparison to physicochemical approaches, formation of silver NPs offers advantages such as cost-effectiveness, environmental friendliness, ease of scaling up, and lack of need for toxic chemicals, high energy, or temperatures (Nie *et al.*, 2018).

Latent building blocks for electronic, optoelectronic, pharmaceutical, and other products, including solar cells, have been produced by recent advances in nanotechnology and nanoscience (Tortella *et al.*, 2020). Shampoos, soaps, detergents, cosmetics, and toothpaste are just a few examples of goods where expensive metal NPs like gold (Au), silver (Ag), platinum (Pt), and copper (Cu) are frequently utilized, in addition to applications in medicine and pharmaceuticals. Based on their capabilities in electromagnetic, photonic, chemical, and mechanical sectors, nanoparticles are currently used in a variety of fields, including the medical field for drug delivery, antimicrobial technology, and diagnosis, and also the electronic and optoelectronic industries (Teodoro *et al.*, 2019; Panáček *et al.*, 2018) in the chemical sector for catalysis (Ananthi *et al.*, 2020) for environmental protection (Zannotti *et al.*, 2020) and energy adaptation (Anwar *et al.*, 2018). The most of physicochemical processes used to produce nanoparticles particular nanoparticles, such as pyrolysis, chemical or physical vapor deposition, lithography electro-deposition, etc., are not ecologically friendly (Zhang *et al.*, 2020). There have been various cases of the creation of nanoparticles such ZnO, CdO, NiO, and Sm₂O₃ (Vorobyev *et al.*, 2020; Chen *et al.*, 2020; Torras *et al.*, 2020). Commercial approaches have been demonstrated to be useful tools for synthesis, but given the use of potentially toxic substances and the possibility for the development of toxic byproducts in some situations, prolonged use of these methods could be detrimental to both the environment and human well-being (Blanco-Formoso *et al.*, 2020).

Silver is preferred over other noble metals for nanoparticles because of its ability to catalyze antimicrobial reactions and because it is harmless to humans (Farooq *et al.*, 2019). Unlike other metals, AgNPs have been created utilizing a variety of methods, such as physicochemical and biological ones. Silver nanoparticles were previously produced via harmful processes that used dangerous chemicals. Thus, "bio synthesis" prefers to utilize environmentally acceptable technologies for the manufacture of silver nanoparticles. Because it can easily be upscaled for large-scale production and doesn't require dangerous chemicals, extreme pressure, extreme heat, or energy, biosynthesis is preferred to standard synthesis. It simply requires one step, costs less money, and respects the environment (Jiang *et al.*, 2020). Numerous scientists have revealed the utilization of materials such as plant extracts (leaf, latex, stem, seed, root), fungus, bacteria and enzymes in order to generate silver nanoparticles, because they are antioxidants and can lower metallic constituents in the corresponding nanoparticles (Adhikary *et al.*, 2018). Plant extracts are used to create a great capped component for stabilizing AgNPs (Ahmed *et al.*, 2016).

There are 35 different species of the Verbenaceae family plant *Duranta*. It is a native plant of Asia, Africa, and America (Kubasheva *et al.*, 2020). Commonly referred to as "golden dewdrop," *Duranta erecta* (also known as *D. repens*) is an upright, writhing shrub that grows to a height of one to three metres. It is planted as a decorative or as a fence plant in several regions of Ghana. The genus *Duranta* has given rise to coumarinolignoids, cinnamic acid, lamiide, and p-methoxycinnamic acid as phytoconstituents (Jadhav *et al.*, 2018; Mohanta *et al.*, 2020). Numerous bioactive compounds like acetone, raffinose, dextrose, and lamiide have now been successfully identified from *Duranta repens* (Singh *et al.*, 2018). The plant's several parts can be used to heal a variety of diseases. (Leaves and fruit are sometimes used as vermifuges or diuretics and are utilized in traditional folk medicine to treat abscesses, intestinal worms, and malaria. According to reports, *D. erecta* has potent antibacterial and anticancerous properties (Hemlata *et al.*, 2020). One of its numerous natural uses is as an insecticide and antifungal (Ekenma *et al.*, 2018). According to reports, *Plasmodium falciparum* isolates that were chloroquine-effective and resistant were strongly inhibited by ethyl acetate leaf extract. *Aspergillus flavus*, *Rhizopus* sp., *Penicillium*, *Alternaria* sp., and *Trichoderma* sp. were all resistant to the antifungal effects of methanolic extracts of *D. erecta*'s various components, including the leaves, stem, seed and roots (Oluwafemi *et al.*, 2019). There are numerous uses for the entire plant. For instance, the leaf is used to heal abscesses, while the fruits are utilized as a febrifuge to treat intestinal worms and malaria. The entire plant is used in Bangladesh by both the tribal and urban populations as an insect repellent and a remedy for itching, infertility, fever, and pneumonia. It was believed that flowers were stimulants. *D. erecta* is said to possess diuretic qualities that can be used to help the body drain kidney stones out (Vanti *et al.*, 2019). To the aimed to contribute, no such in vitro or in vivo research have been conducted as of yet, according to a review of the literature. We worked on the formation of AgNPs and detailed them in the current work using UV-Visible spectroscopy, XRD, TEM, and FT-IR. In the current study, fresh *D. erecta* leaf extracts have been utilized to synthesise silver NPs, which were then investigated for their antibacterial properties against a variety of pathogenic microorganisms.

MATERIAL AND METHODS

Sample collection:

Duranta erecta L. fresh leaves were collected from the Botanical garden of Sheth M.N. Science College located in Patan, Gujarat, India (Location: 23°86'12" N 72°13'03" E). Identification and authentication of *D. erecta* were done using e-flora of India.

Preparation of leaf extract:

Aqueous leaf extract from the sample's freshly harvested 5g of *D. erecta* leaves was created, and it was afterwards cleaned twice with water that had undergone double distillation. The leaves were then cooked for five minutes at 60° C with 100 milliliters of filtered water (Kathireswari *et al.*, 2014). Before being centrifuged for 25 minutes at 7,000 rpm, the mixture was filtered using Whatman filter paper no. 1. The leaf extract was placed in a cold storage at 4° C to be used later.

Synthesis of Silver nanoparticles:

Silver nanoparticles were formed by synthesizing silver nitrate (AgNO_3) in aqueous solution at a 1 mM concentration. 90 ml of an aqueous solution containing 1 mM silver nitrate (AgNO_3) and 10 ml of *D. erecta* leaf extract were used to convert Ag^0 to Ag^+ ions (Murugan and Shanmugasundaram, 2014). Through colour perception, the visual analysis of embedded silver nanoparticles was recorded. Centrifugation was used to collect the AgNPs for 15 min at 10,000 rpm. To get rid of the unconverted metal ions, distilled water was used to wash the collected pellet. The mixture was stored in a cold storage to be used for further spectral analysis and antibacterial activity.

Characterizations of AgNPs:

The UV-Vis spectra of AgNPs reaction mixture aliquots were observed dependent on SPR as a function of response time inside 190-1100 nm frequencies with a resolution of 1 nm using a UV-visible spectrophotometer (UV-1800 SHIMADZU, Double-beam Spectrophotometer). A powder X-ray diffractometer (X'pert Pro, PANalytical Netherlands) was used to record XRD for drop-covered air-dried samples on glass substrate at 5° to 140° 2 θ with Nickel beta filter and CuK radiation source on 1.54 Å wavelength in order to examine the crystalline structure of the purified AgNPs. Using a Perkin Elmer instrument, USA, plant extract and AgNPs FTIR spectra were obtained spanning the 4000-400 cm^{-1} range from 24 scans with a resolution at 0.4 cm^{-1} . To evaluate the characteristics (size, morphology and shape) of AgNPs, H-7500 Hitachi, Japan, performed TEM with a 40-120 kV operating voltage and a 0.36 nm resolution.

Antibacterial activity of silver nanoparticles:

The antibacterial study changed into dictated by the agar well technique. As test organisms for the antibacterial activity, the gram-negative bacteria *Pseudomonas aeruginosa*, *Escherichia coli*, and the gram-positive microorganisms *Staphylococcus aureus* and *Bacillus subtilis* were used. Nutrient agar slants had been used to cultivate the bacterial strains. Sub-culturing was used to maintain the cultures on a regular basis, and they were stored at 4°C until further usage. Antibacterial activity in opposition to the pathogenic bacterial strains made in different appositeness of antibacterial action with a concentration of 50 μl , 60 μl , and 70 μl compared with the positive standard (Chloramphenicol-30 μl) and negative control (distilled water). The widths of the inhibited zone surrounding each well were measured following a 24-hour incubation period at 37°C in a bacteriological incubator.

RESULTS

UV-Vis spectra analysis:

Metal nanoparticles' distinctive SPR imaging pattern is determined using UV-visible spectroscopy. The initial optical confirmation of the AgNPs synthesis came from the visible portion of the reaction mixture's colour change to brown. The yellow aqueous leaf extract (A) was combined with the silver nitrate solution and simmered for ten minutes at 60°C. The colour transformation to brown (C) defined that AgNPs had formed (Fig 1). This colour change was caused by a number of biomolecules in the leaf extract that converted Ag⁺ to Ag⁰. Figure 2 displays the Uv-vis spectra in *D. erecta* that were captured 30 minutes, 3 hours, and 24 hours after the response started. By lengthening the response time, the colour intensity was expanded. This colour change was caused by a number of biomolecules in the leaf extract that converted Ag⁺ to Ag⁰. The development of silver nanoparticles was periodically monitored using UV-Vis spectroscopy. In the instance of a *D. erecta* leaf, the steep peak of silver nanoparticles was seen at about 410 nm, as indicated in Fig 3.

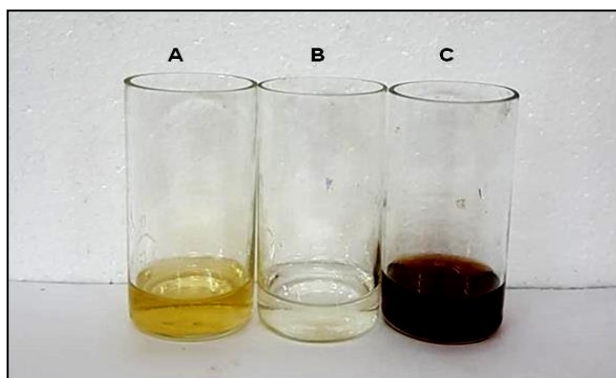


Fig. 1. Visual observation (A) *D. erecta* Leaf extracts (B) AgNO₃ solution (C) AgNPs



Fig 2. Different time interval colour intensity of *D. erecta* leaf extract AgNPs

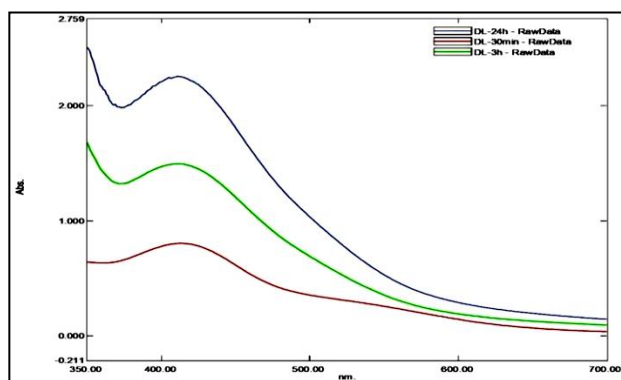


Fig 3. UV-visible spectra of *D. erecta* AgNPs obtained using leaf extract

X-ray diffraction Analysis:

To examine the crystallographic structure of the pure *D. erecta* AgNPs, the X-ray diffractometer (XRD) was employed to record 2 scans from 10° to 90° at 0.01° per min with such a time steady of 2s on glass substrate. Powder XRD was initially employed to analyze the crystalline structure of the *D. erecta* AgNPs, as shown in Fig. 4. At $2\theta = 38.23^\circ$, 44.38° , 64.58° , and 77.46° , which correspond to the (111), (200), (220), and (311) planes of FCC structures, respectively, Bragg's reflections had been seen. The parameters that were established using the XRD analysis of AgNPs are shown in Table 1. This is confirmed by the common metallic silver XRD pattern JCPDS No. 04-0873. XRD also found a couple very strong peaks, however they were not labeled in Fig 4. According to this theory, the extra peaks are the result of the bioorganic phase crystallizing on the AgNPs-interface. The UV and FT-IR studies as well as the TEM clearly demonstrate this.

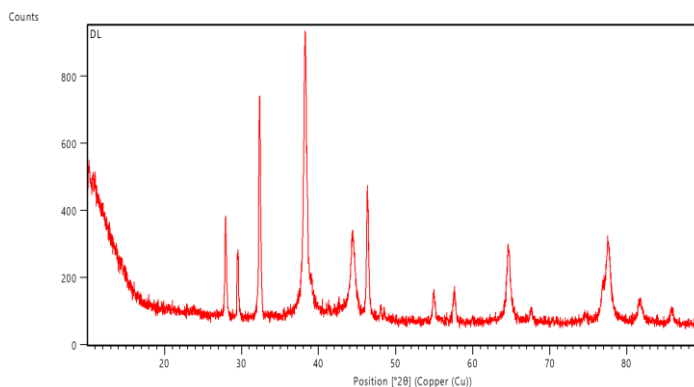


Fig 4. XRD pattern of synthesized AgNPs using the leaf extract of *D. Erecta*

Table 1. Different parameters of the XRD analysis of AgNPs of *D. erecta* leaf extract

2θ (Degree)	FWHM	Diffraction plane (hk1)	Interplanar spacing "d"	Crystallite size (nm)
38.15°	0.41	111	2.35	21.42
44.38°	0.67	200	2.03	13.38
64.58°	0.47	220	1.44	14.66
77.46°	0.61	311	1.23	17.45

Fourier Transform Infrared (FTIR) Spectroscopy Analysis:

The chemical components used to create *D. erecta* AgNPs are examined using FT-IR spectroscopy. In order to pinpoint the several functional groups involved for changing silver nitrate into silver nanoparticles, AgNPs were applied in powder form for the experiment. The leaf extract peak values in the FTIR spectrum were 3341.08 cm^{-1} , 2117.46 cm^{-1} , 1635.74 cm^{-1} , 611.95 cm^{-1} , and 523.43 cm^{-1} , as shown in Fig. 5. Alkyl halides' O-H stretching vibrations are represented by the band at 3341.08 cm^{-1} , alkynes are represented by the band at 2117.46 cm^{-1} , alkenes are represented by the band at 1635.74 cm^{-1} , and C-Br stretching vibrations are represented by the band at 611.95 cm^{-1} and 523.43 cm^{-1} , respectively. The FTIR spectrum, as shown in Fig. 6, has a number of distinct peaks. To understand the biomolecules for capping and effective stability of the generated metallic nanoparticles, FTIR analyses were conducted. The intensity peaks of 3912.31 cm^{-1} , 3760.10 cm^{-1} , 3459.17 cm^{-1} , 2424.42 cm^{-1} , and 2069.61 cm^{-1} are somewhat raised throughout this time, whereas other intensity peaks, including 1633.06 cm^{-1} , 1121.21 cm^{-1} , and 579.15 cm^{-1} , are slightly decreased. The band in Fig. 6 corresponds to alcohol's O-H stretching vibrations at 3464.79 cm^{-1} . C-N alkenes are represented by the peak at 2424.42 cm^{-1} , C=C alkenes are represented by the peak at 1633.06 cm^{-1} , and aldehydes and ketones are represented by the peak at 1121.21 cm^{-1} . Alkyl halides' C-H, C-Br stretching vibrations account for the peak at 579.15 cm^{-1} .

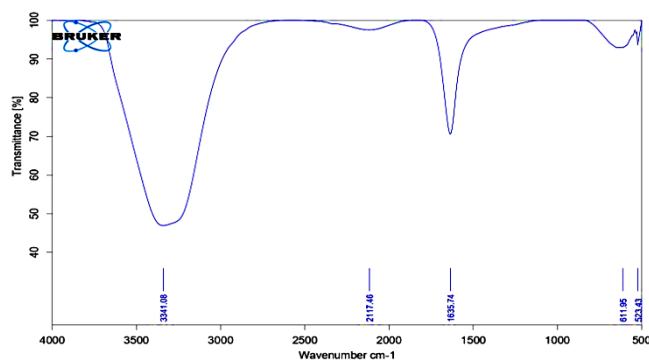


Fig 5. FTIR spectra of *D. erecta* leaf extract

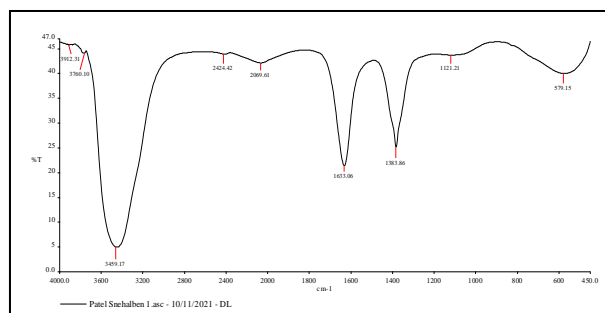


Fig 6. FTIR spectra of synthesized AgNPs of *D. erecta* leaf extract

TEM Analysis:

The size, morphology, and form of nanoparticles have all been determined utilizing transmission electron microscopy. Although some of the silver nanoparticles were found to have irregular shapes, as seen in Fig. 7, it shows that the silver nanoparticles are highly distributed and generally sphere-shaped. According to the form of the SPR band in the UV-visible spectrum, the nanoparticles are homogeneous and spherical. Figures also show a variation in particle size and size distribution. Particle size ranges from 6 to 8 nm, with an average measurement of 7 nm.

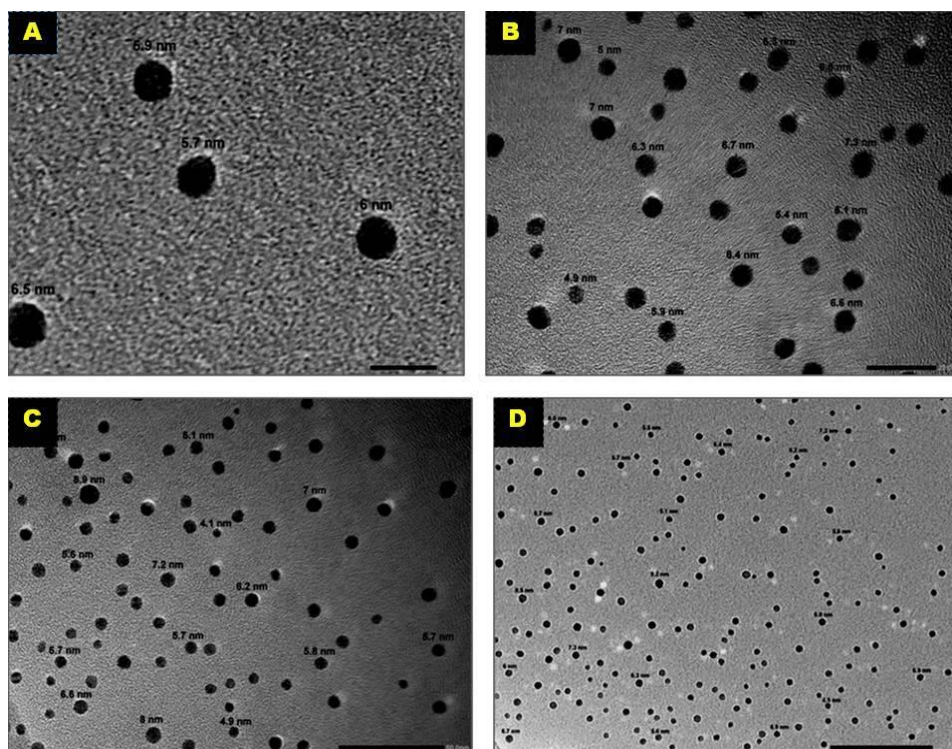


Fig 7. Transmission electron microscopy (TEM) images of AgNPs by *D. erecta* (A) 10 nm (B) 20 nm (C) 50 nm (D) 100 nm

Antibacterial activity

the silver nanoparticles' antibacterial properties, which were created using *D. erecta* leaf extracts. Through using the agar disk diffusion method, the antibacterial efficacy of green-generated AgNPs was examined against a variety of pathogenic species, including Gram-positive microbes (*B. subtilis* & *S.aureus*) and Gram-negative microbes (*P. aeruginosa* & *E. coli*). The triple of breadth's mean inhibition zone was identified and summarised (Fig. 8). *E. coli* was discovered to be the most effective pathogen examined, and the significant bacterial inhibitory action of *D. erecta* leaf extract-mediated AgNPs was identified concentration-dependently. As seen in Table 2, the zone of inhibition (ZOI) grew with increasing AgNP concentrations. Gram-negative microbe *Escherichia coli* exhibits the highest zone of inhibition ($24.00 \pm 0.58 \text{ mm}$) by AgNPs made from *D. erecta* leaf extracts, preceded by Gram-negative *P. aeruginosa* ($21.00 \pm 28 \text{ mm}$), Gram-positive *Staphylococcus aureus* ($21.33 \pm 0.11 \text{ mm}$), and Gram-positive *Bacillus subtilis* ($20.17 \pm 0.28 \text{ mm}$) at a concentration of $70 \mu\text{l}$, as can be seen in table 2.

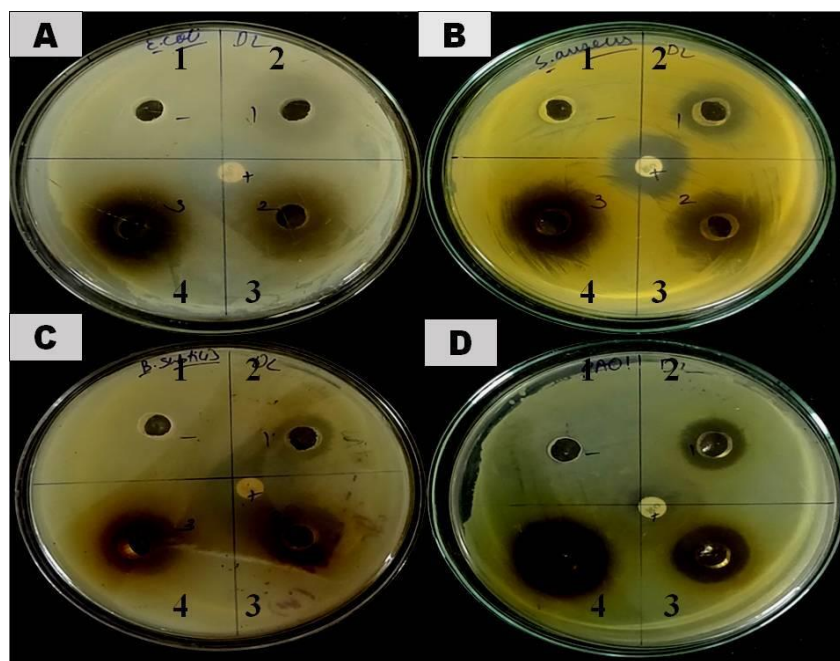


Fig 8. Antibacterial activity of *D. erecta* -AgNPs prepared by *D. erecta* leaf extract against (A) *Escherichia coli* (B) *Staphylococcus aureus* (C) *Bacillus subtilis* (D) *Pseudomonas aeruginosa*
Note: 1= Negative Control, 2= Plant extract, 3=AgNO₃, 4= AgNPs

(NOTE: Values are the mean of three replicates ± standard error.)

Table 2. Antibacterial activity of AgNPs synthesized by using *D. erecta* leaf extract

Bacteria Class	Name of the organism	Concentrations (µl)	Zone of Inhibition(mm)		
			Plant extract	Silver nitrate (AgNO ₃)	Silver nanoparticles DL
Gram negative	<i>Escherichia coli</i>	50 µl	15.33±0.33	15.31±0.33	17.23±0.33
		60 µl	16.33±0.33	18.13±0.33	19.20±0.33
		70 µl	18.00±0.58	21.11±0.58	24.20±0.58
	<i>Pseudomonas aeruginosa</i>	50 µl	13.63±0.44	14.83±0.44	17.03±0.44
		60 µl	14.87±0.20	16.07±0.20	19.37±0.20
		70 µl	15.00±0.28	17.05±0.28	21.00±0.28
Gram positive	<i>Bacillus subtilis</i>	50 µl	10.66±0.35	14.54±0.35	16.23±0.35
		60 µl	12.27±0.64	16.29±0.64	18.19±0.64
		70 µl	13.50±0.28	18.10±0.28	20.17±0.28
	<i>Staphylococcus aureus</i>	50 µl	14.19±0.34	16.63±0.34	18.50±0.34
		60 µl	15.12±0.06	17.09±0.06	19.42±0.06
		70 µl	16.00±0.11	19.09±0.11	21.33±0.11

DISCUSSION

The varied portions of plant extracts are eco-friendly, affordable, and nontoxic for the creation of NPs. The utilization of leaf extract for the formation of NPs has the added advantage of being ecologically beneficial. Since leaves are typically readily available in large quantities, it is a great idea to consider their potential for healing. The current research aimed to synthesize nanoparticles from *D. erecta* leaf extract. Standardization of the combination of extract amount and boiling duration for the production of plant extract was done for the production of silver NPs. The aqueous leaves extract of *D. erecta* was employed to make AgNPs, and as a result, the solution's colour changed from pale yellow to dark brown. At 410 nm, the surface plasma resonance (SPR) was monitored, which shows that AgNPs were produced. During an experimental period, the SPR peak was assumed to have been enhanced due to increased NP production. As more nanoparticles are created as a result of the phytochemical compounds in *D. erecta* leaf extract decreasing the silver ions in the aqueous solution, the intensity may have increased. Over a period of 2.5 months, the stability of produced AgNPs was observed and documented. AgNPs agglomeration or SPR changes weren't found during storage. The generation of AgNPs was also quite stable over the course of subsequent

tests, and this stability may be useful in a variety of therapeutic applications. The SPR peak in the visible range at 404 nm in *D. erecta* formed after 30 minutes and became more apparent over time. The SPR peak grew stronger with longer reaction times, indicating the formation of metallic silver nanoparticles. In the production of AgNPs from the leaf of *D. erecta*, the SPR peak obtained approximately 410 nm (Raj *et al.*, 2018), and 423 nm peak value occurred in the *V.negundo* leaf portion (Feroze *et al.*, 2020), which was as comparable as in the current investigation. XRD measurement confirmed that silver nanoparticles were crystalline in form. In countless more investigations on the synthesis of AgNPs using various extracts, extra peaks were also found. For instance, AgNPs generated from *Azadirachta indica* leaf extract showed numerous distinct peaks in the diffractogram (Hamouda *et al.*, 2019). Similar works are done in various plants such; The XRD pattern was utilized to establish that the synthesized AgNPs are found to be very stable with the crystalline character. The XRD spectrum analysis found two separate diffraction peaks at 38.08°, and 43.47°; it has been indexed as (111), (200) in *Capparis* leaves extract (Samuel *et al.*, 2020).

Understanding the role of functional groups in the interaction between metallic particles and biomolecules is now possible due to the advancement of FTIR technology. It is utilized to identify the biomolecules required for capping and effective longevity of the metallic nanoparticles and examine the chemical elements of the surface of AgNPs. There were various functional groups present like Alkynes, Alkenes, Halides, which may have been responsible for the bio-reduction of Ag⁺ ions. Different bond strains can be seen in the FTIR analysis results at various peaks, including the 3432.94 for N-H stretch, 2777.28 for single aldehydes, 2676.19 for C-H, 2071.75 for CC, 1637.58 for C=C, and 1121.56 for C=O, which are assigned to OH stretching and aldehydes C-H stretching, respectively (Ibrahim *et al.*, 2019). Assimilation bands were visible in the spectrum at 3419, 2927, 1625, 1383, 1069, and 602 cm⁻¹. The peaks at 3419 cm⁻¹ matched to -OH stretching because of the phenolic compounds present in the extract of phlomis leaf (Vanlalveni *et al.*, 2018). Using TEM, it was possible to see how big and how spherical the produced AgNPs were. These biosynthesized silver nanoparticles are almost the same size as previously reported biologically synthesized AgNPs made from *Coleus* leaf, 40-50 nm, living peanut seedling, 30-100 nm (Fouda *et al.*, 2020), *Petroselinum* leaf extract, 30-32 nm (Cai *et al.*, 2019) etc. The findings of the current investigation clearly revealed that antibacterial activity was stronger when antibiotics plus AgNPs were employed than when antibiotics plus acetone extract was utilized, as evidenced by increase in zone area. The AgNPs successfully suppressed Gram negative bacteria, even better than acetone extract. The mechanism of inhibitory actions of silver ions on microorganisms is relatively recognized. AgNPs biosynthesized from *Bambusa vulgaris* leaves also demonstrate excellent anti-microbial effects against sample bacteria cultures (Brito *et al.*, 2020). The anti-microbial inhibitory action in *Morinda citrifolia* leaf extract and findings showed that Synthesized Silver nanoparticles against the human diseases such as *S. aureus* and *P. aeruginosa* strains suggested the development of pathogenic resistance (Saratale *et al.*, 2020).

CONCLUSION

The leaf extract of *D. erecta* was successfully used to produce silver nanoparticles utilizing a plant-mediated, environmentally friendly method. It was discovered that the various biomolecules included in the leaf extract were in charge of producing and maintaining the NPs. UV-Vis spectroscopy, XRD, FTIR, and TEM were used to illustrate the size, shape, crystalline structure, and stability. Fourier Transform Infrared Spectroscopy was used to evaluate the FCC structure and functional groups present in the nanoparticles, while X-ray diffraction and TEM were used to confirm an average size of 6 to 16 nm (FTIR). It turns out to be an efficient, green synthesis method that is eco-friendly, providing a realistic and affordable method for the creation of AgNPs. The NPs created in the current work showed antibacterial activity against specific pathogens, which indicated that they may be involved in the creation of future medications. With the potential to be used in biomedical applications and expected to play a key role in optoelectronics and medical devices in the near future, this environmentally friendly approach may be a competitive alternative to the typical physical/chemical approaches used for the production of AgNPs.

Competing interests

The authors declare that they have no competing interests.

Funding

This research work received no external funding.

Authors' contributions

S.P. conceived the experiments, performed the experiments, analyzed the data and wrote the article. N.K. conceived the experiments, provided and facility supports, discussed the results. All authors have read and agreed to the published version of the manuscript.

Acknowledgements

The authors wish to express their thanks to principal of Sheth M.N. Science College, Patan for providing a lab facility to explore this research work. Authors also acknowledge the SAIF, Chandigarh, Panjab University for FTIR, XRD and TEM analysis.

REFERENCES

- Adhikary, J., Meyerstein, D., Marks, V., Meistelman, M., Gershinsky, G., Burg, A., ... & Albo, Y. (2018). Sol-gel entrapped Au⁰- and Ag⁰-nanoparticles catalyze reductive de-halogenation of halo-organic compounds by BH₄⁻. *Applied Catalysis B: Environmental*, 239, 450-462.
- Ananthi, V., Prakash, G. S., Rasu, K. M., Gangadevi, K., Boobalan, T., Raja, R., ... & Arun, A. (2018). Comparison of integrated sustainable biodiesel and antibacterial nano silver production by microalgal and yeast isolates. *Journal of Photochemistry and Photobiology B: Biology*, 186, 232-242.

- Anwar, A., Siddiqui, R., Hussain, M. A., Ahmed, D., Shah, M. R., & Khan, N. A. (2018). Silver nanoparticle conjugation affects antiacanthamoebic activities of amphotericin B, nystatin, and fluconazole. *Parasitology research*, *117*(1), 265-271.
- Blanco-Formoso, M., Turino, M., Rivas-Murias, B., Guerrini, L., Shavel, A., de la Rica, R., ... & Alvarez-Puebla, R. A. (2020). Iron-assisted synthesis of highly monodispersed and magnetic citrate-stabilized small silver nanoparticles. *The Journal of Physical Chemistry C*, *124*(5), 3270-3276.
- Brito, T. K., Viana, R. L. S., Moreno, C. J. G., da Silva Barbosa, J., de Sousa Júnior, F. L., de Medeiros, M. J. C., ... & Rocha, H. A. O. (2020). Synthesis of silver nanoparticle employing corn cob xylan as a reducing agent with anti-Trypanosoma cruzi activity. *International Journal of Nanomedicine*, *15*, 965.
- Cai, Z., Dai, Q., Guo, Y., Wei, Y., Wu, M., & Zhang, H. (2019). Glycyrrhiza polysaccharide-mediated synthesis of silver nanoparticles and their use for the preparation of nanocomposite curdlan antibacterial film. *International journal of biological macromolecules*, *141*, 422-430.
- Chen, S., Drehmel, J. R., & Penn, R. L. (2020). Facile synthesis of monodispersed Ag NPs in ethylene glycol using mixed capping agents. *ACS omega*, *5*(11), 6069-6073.
- Ekenma A.J., Ejikene O.D., Ekeh F., Uwagbae M., Ngwu G., and Ehilegbu C. (2018). Bioefficacy of *Duranta erecta* extract on yellow fever and dengue vector, *Aedes aegypti* Linn. in Nigeria, *Journal of Medicinal Plants Research*, *12*(11), 124–132.
- Farooq, U., Ahmad, T., Khan, A., Sarwar, R., Shafiq, J., Raza, Y., ... & Al-Harrasi, A. (2019). Rifampicin conjugated silver nanoparticles: a new arena for development of antibiofilm potential against methicillin resistant Staphylococcus aureus and Klebsiella pneumoniae. *International Journal of Nanomedicine*, *14*, 3983.
- Feroze, N., Arshad, B., Younas, M., Afridi, M. I., Saqib, S., & Ayaz, A. (2020). Fungal mediated synthesis of silver nanoparticles and evaluation of antibacterial activity. *Microscopy Research and Technique*, *83*(1), 72-80.
- Fouda, M. M., Abdelsalam, N. R., El-Naggar, M. E., Zaitoun, A. F., Salim, B. M., Bin-Jumah, M., ... & Kandil, E. E. (2020). Impact of high throughput green synthesized silver nanoparticles on agronomic traits of onion. *International journal of biological macromolecules*, *149*, 1304-1317.
- Hamouda, R. A., Hussein, M. H., Abo-Elmagd, R. A., & Bawazir, S. S. (2019). Synthesis and biological characterization of silver nanoparticles derived from the cyanobacterium Oscillatoria limnetica. *Scientific reports*, *9*(1), 1-17.
- Hemlata, Meena, P. R., Singh, A. P., & Tejavath, K. K. (2020). Biosynthesis of silver nanoparticles using Cucumis prophetarum aqueous leaf extract and their antibacterial and antiproliferative activity against cancer cell lines. *ACS omega*, *5*(10), 5520-5528.
- Ibrahim, E., Fouad, H., Zhang, M., Zhang, Y., Qiu, W., Yan, C., ... & Chen, J. (2019). Biosynthesis of silver nanoparticles using endophytic bacteria and their role in inhibition of rice pathogenic bacteria and plant growth promotion. *RSC advances*, *9*(50), 29293-29299.
- Jadhav, K., Deore, S., Dhamecha, D., Hr, R., Jagwani, S., Jalalpure, S., & Bohara, R. (2018). Phytosynthesis of silver nanoparticles: characterization, biocompatibility studies, and anticancer activity. *ACS Biomaterials Science & Engineering*, *4*(3), 892-899.
- Jiang, L., Santiago, I., & Foord, J. (2020). High-yield electrochemical synthesis of silver nanoparticles by enzyme-modified boron-doped diamond electrodes. *Langmuir*, *36*(22), 6089-6094.
- Jouyban, A., & Rahimpour, E. (2020). Optical sensors based on silver nanoparticles for determination of pharmaceuticals: An overview of advances in the last decade. *Talanta*, *217*, 121071.
- Kathireswari P., Gomathi S. and Saminathan K. (2014). Plant leaf mediated synthesis of silver nanoparticles using Phyllanthus niruri and its antimicrobial activity against multi drug resistant human pathogens. *International Journal of Current Microbiology and Applied Sciences*, *3*(3), 960-968.
- Kubasheva, Z., Sprynskyy, M., Railean-Plugaru, V., Pomastowski, P., Ospanova, A., & Buszewski, B. (2020). Synthesis and antibacterial activity of (AgCl, Ag) NPs/diatomite hybrid composite. *Materials*, *13*(15), 3409.
- Liu, Y., Li, F., Guo, Z., Xiao, Y., Zhang, Y., Sun, X., ... & Wang, J. (2020). Silver nanoparticle-embedded hydrogel as a photothermal platform for combating bacterial infections. *Chemical Engineering Journal*, *382*, 122990.
- Mohanta, Y. K., Biswas, K., Jena, S. K., Hashem, A., Abd_Allah, E. F., & Mohanta, T. K. (2020). Anti-biofilm and antibacterial activities of silver nanoparticles synthesized by the reducing activity of phytoconstituents present in the Indian medicinal plants. *Frontiers in Microbiology*, *11*, 1143.
- Murugan A. and Shanmugasundaram K. (2014). In vitro: Phytochemical screening and evaluation of antioxidant potential of Vitex negundo Linn. Of synthesized Silver nanoparticles, *world journal pharmacy and pharmaceutical science*, *3*(8), 1385-1393
- Nie, W., Dai, X., Li, D., McCoul, D., Gillispie, G. J., Zhang, Y., ... & He, C. (2018). One-pot synthesis of silver nanoparticle incorporated mesoporous silica granules for hemorrhage control and antibacterial treatment. *ACS Biomaterials Science & Engineering*, *4*(10), 3588-3599.
- Oluwafemi, O. S., Anyik, J. L., & Zikalala, N. E. (2019). Biosynthesis of silver nanoparticles from water hyacinth plant leaves extract for colourimetric sensing of heavy metals. *Nano-Structures & Nano-Objects*, *20*, 100387.
- Panáček, A., Kvítek, L., Smékalová, M., Večeřová, R., Kolář, M., Röderová, M., ... & Zbořil, R. (2018). Bacterial resistance to silver nanoparticles and how to overcome it. *Nature nanotechnology*, *13*(1), 65-71.
- Raj, S., Mali, S. C., & Trivedi, R. (2018). Green synthesis and characterization of silver nanoparticles using Enicostemma axillare (Lam.) leaf extract. *Biochemical and biophysical research communications*, *503*(4), 2814-2819.
- Samuel, M. S., Jose, S., Selvarajan, E., Mathimani, T., & Pugazhendhi, A. (2020). Biosynthesized silver nanoparticles using Bacillus amyloliquefaciens; Application for cytotoxicity effect on A549 cell line and photocatalytic degradation of p-nitrophenol. *Journal of Photochemistry and Photobiology B: Biology*, *202*, 111642.

- Saratale, G. D., Saratale, R. G., Kim, D. S., Kim, D. Y., & Shin, H. S. (2020). Exploiting fruit waste grape pomace for silver nanoparticles synthesis, assessing their antioxidant, antidiabetic potential and antibacterial activity against human pathogens: a novel approach. *Nanomaterials*, 10(8), 1457.
- Siddiqi, K. S., Husen, A., & Rao, R. A. (2018). A review on biosynthesis of silver nanoparticles and their biocidal properties. *Journal of nanobiotechnology*, 16(1), 1-28.
- Singh, P., Pandit, S., Garnaes, J., Tunjic, S., Mokkalapati, V. R. S. S., Sultan, A., ... & Mijakovic, I. (2018). Green synthesis of gold and silver nanoparticles from Cannabis sativa (industrial hemp) and their capacity for biofilm inhibition. *International journal of nanomedicine*, 13, 3571-3591.
- Teodoro, K. B., Shimizu, F. M., Scagion, V. P., & Correa, D. S. (2019). Ternary nanocomposites based on cellulose nanowhiskers, silver nanoparticles and electrospun nanofibers: Use in an electronic tongue for heavy metal detection. *Sensors and Actuators B: Chemical*, 290, 387-395.
- Torras, M., & Roig, A. (2020). From silver plates to spherical nanoparticles: snapshots of microwave-assisted polyol synthesis. *ACS omega*, 5(11), 5731-5738.
- Tortella, G. R., Rubilar, O., Durán, N., Diez, M. C., Martínez, M., Parada, J., & Seabra, A. B. (2020). Silver nanoparticles: Toxicity in model organisms as an overview of its hazard for human health and the environment. *Journal of hazardous materials*, 390, 121974.
- Vanlalveni, C., Rajkumari, K., Biswas, A., Adhikari, P. P., Lalfakzuala, R., & Rokhum, L. (2018). Green synthesis of silver nanoparticles using Nostoc linckia and its antimicrobial activity: a novel biological approach. *BioNanoScience*, 8(2), 624-631.
- Vanti, G. L., Nargund, V. B., Vanarchi, R., Kurjogi, M., Mulla, S. I., Tubaki, S., & Patil, R. R. (2019). Synthesis of Gossypium hirsutum-derived silver nanoparticles and their antibacterial efficacy against plant pathogens. *Applied Organometallic Chemistry*, 33(1), e4630.
- Vorobyev, S. A., Likhatski, M. N., Romanchenko, A. S., Fetisova, O. Y., Kazachenko, A. S., Volochaev, M. N., & Mikhlin, Y. L. (2020). Fabrication of extremely concentrated silver hydrosols without additional stabilizers. *ACS Sustainable Chemistry & Engineering*, 8(46), 17225-17233.
- Yang, L., Zhen, S. J., Li, Y. F., & Huang, C. Z. (2018). Silver nanoparticles deposited on graphene oxide for ultrasensitive surface-enhanced Raman scattering immunoassay of cancer biomarker. *Nanoscale*, 10(25), 11942-11947.
- Zannotti, M., Vicomandi, V., Rossi, A., Minicucci, M., Ferraro, S., Petetta, L., & Giovannetti, R. (2020). Tuning of hydrogen peroxide etching during the synthesis of silver nanoparticles. An application of triangular nanoplates as plasmon sensors for Hg²⁺ in aqueous solution. *Journal of Molecular Liquids*, 309, 113238.
- Zhang, X., Chen, Z., & Zuo, X. (2020). Chloroauric acid/silver nanoparticle colorimetric sensors for antioxidant discrimination based on a honeycomb Ag-Au nanostructure. *ACS Sustainable Chemistry & Engineering*, 8(9), 3922-3928.

